Preceramic Polymers as Laminating Systems for the Fabrication of Tape-Cast AlN Multilayer Components

Abstract

Laminating pastes used for the fabrication of tape-cast multilayer components usually contain organic binder systems with inorganic fillers. Microstructural changes in the laminating pastes lead often to differences in the multilayer components. Tests with preceramic polymers (Trimethyliminoalane) were done. A description of the paste preparation and paste composition as well as the manufacturing process is given. Components produced did not exhibit any differences in mirostructures after sintering.

Introduction

With its interesting combination of properties, including high thermal conductivity, high electrical resistance, low dielectric permittivity, low coefficient of thermal expansion and relatively high strength AlN is regarded as a potential material for application in microelectronics and power electronics. In power electronics, for example, the thyristors used for the supply of electric current to German intercity express trains are cooled with water by means of complex heat exchanger structures made of AlN [1]. These complex-shaped components are usually fabricated by means of isostatic pressing with subsequent green machining. To optimize this technique, which is applied particularly for short product runs and large-volume components, considerable effort has gone into the optimization of the binder and adaptation of the machining parameters [2].

However, this process can only be regarded as a makeshift solution, which, while no doubt being important for short product runs and large-volume components, is less expedient for the mass production of complex-shaped components involving large numbers of pieces. Automatic manufacturing processes for rapid fabrication of complex-shaped prototypes and mass production would be possible with the introduction of tape casting. In this process, CAD geometry data are created based on a drawing, a model or a tomographic representation of the component to be fabricated. The component image is then broken down into layers, and working from this image, the component is later built up by the addition of material and the lamination of the individual layers one on top of the other [3]. The tapes can then be structured by punching, laser-cutting or water-jet cutting.

Based on the example of silicon-infiltrated silicon carbide and reaction-bonded silicon nitride, it has been shown that even when characteristic laminating pastes (these are laminating pastes containing an organic binder system and inorganic filler, in this case SiC or Si powder) are used, the properties perpendicular and parallel to the laminating layers differ considerably [4,5]. The laminating layers, which are often applied by screen printing [6], have different microstructural parameters to those of the tape-cast material, and therefore the properties perpendicular and parallel to these laminating layers differ. Also in the thermocompression (bonding of the tapes at elevated temperature and pressure) of the individual tapes with each other, concentrations of organic matter or pores can be detected after burnout. The microstructural changes in the laminating pastes lead to the above-mentioned differences in their properties.

In this research, preceramic polymers (trimethyiminoalane - TMIA) were used as a binder system. After burnout of the residual organic matter, these polymers leave behind AlN particles, which increase the solid concentration in the laminating pastes and thus produce a microstructure comparable to that in the tape (Fig. 1). As TMIA is not available commercially, it was synthesized at the Institute of Non-Metallic Materials at Clausthal University of Technology. This synthesis is described in detail in the work of Seibold, Vierneusel and Rüssel [7-10]. For the laminating tests, AlN tapes supplied by *ANCeram* and *CeramTec* were used.

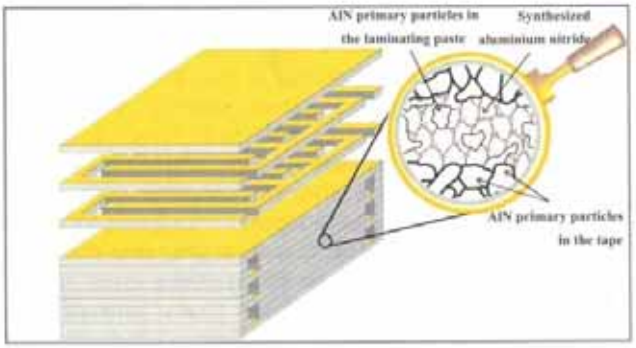

Fig. 1
Aluminium nitride network with aluminium nitride primary particles in the interlayers of an AlN multilayer component -schematic.

Experimental

The electrolysis apparatus was designed based on patent DE 3807419 C2 [10]. The electrode of the electrolysis apparatus (Fig. 2) consists of eight high-purity aluminium sheets measuring (139 x 49 x 1) mm^3. As synthesis must be performed with the exclusion of oxygen, the reaction chamber was flushed continuously with argon. The use of a double-walled glass boiler allowed cooling of the reaction chamber with tap water over the entire duration of the tests, in order to minimize the temperature increase.

The two conducting wires for power supply were connected with a d.c. power pack via a time switch. Owing to the d.c. voltage applied and the required uniform wear of the electrode, the polarity of the power supply was reversed every 30 min. Basis for the synthesis tests was an electrolyte solution with the composition 68,3 mass % n-propylamine, 29,0 mass % acetonitrile and 2,7 mass % tetrabutylammoniumbromide.

Dipl.-Ing. Bernd Bitterlich
Dipl.-Ing. Lars Peters
Dipl.-Ing. Carsten Soldan
Prof. Dr. Jürgen G. Heinrich
TU Clausthal
Institut für Nichtmetallische Werkstoffe
Professur für Ingenieurkeramik
Zehntnerstr. 2a
D-38678 Clausthal-Zellerfeld

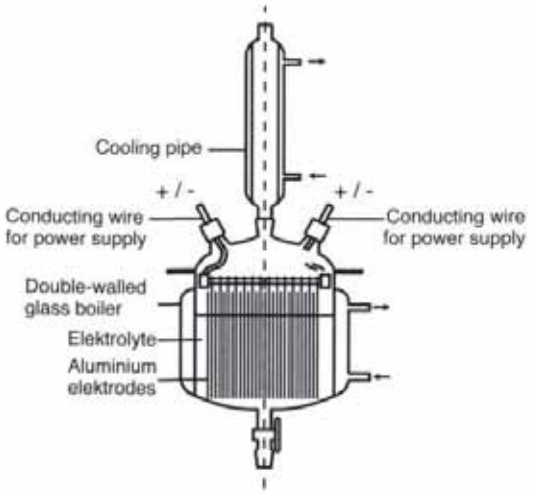

Fig. 2
Set-up of the electrolysis apparatus - schematic.

To prepare the laminating pastes, first the solvent was completely removed from the polymer solutions at 100°C and, at the same time, the polymer was partially cross-linked. The polymer foam formed was placed in a glove box filled with inert gas and comminuted to a fine powder with a mortar. To prepare the laminating liquids, different concentrations of polymer powder were again dissolved in a solvent.

For lamination with pure laminating liquid, the green tapes were first precoated with a 13 h-synthesis solution (Fig. 3). It consisted of the solvents acetonitrile, propylamine and a concentration of around 17 mass % of the AlN precursor TMIA. As a result of the evaporation of the solvent, a thin solid layer of precursor was formed on the green tape. With a solvent-impregnated, lint-free cloth, the precoating was then resolubilized on the surface. Following this resolubilization, the cloth was removed and the green tapes laid on top of each other. With a rubber roller, the tapes were pressed on to each other, in order to eliminate any gas bubbles in the interlayer. Subjected to a loading of around 100 g/cm³, the laminates were stored at room temperature until completely dry, to ensure that the tapes could not delaminate as a result of warpage.

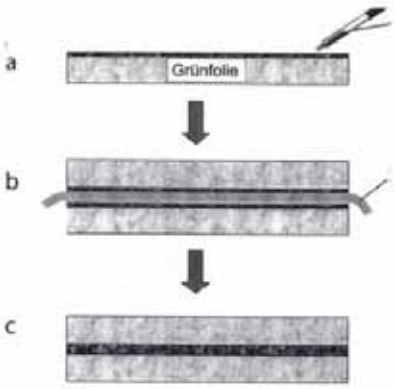

Fig. 3
Schematic showing the laminating process
a) Precoated green tapes
Grünfolie= Green tape
b) Diluted TMIA solution
Solubilization of the coating with an solvent-impregnated cloth
c) Laminate

For larger layer thicknesses, a simple screen and manual squeegee set-up were used to print the pastes on to the tapes. The screen (mesh 200) has a mesh width of 90 mm, with stainless steel wires of 40 µm in diameter. Theoretically, a wet layer thickness of 40...50 µm can be printed with this screen. For production of the screen printing pastes, formamides were used as solvents. Their functional group consists of [=N-C=O]. The cross-linked polymer can be dissolved very well in the dimethylformamide (DMF). Owing to the high evaporation rate of DMF, the pastes were made up with a mixture of dimethylformamide and formamide (FA) as its vapour pressure is only 0,08 hPa [11] (for comparison, terpineol, which is often used for screen printing, but which would react chemically with the precursor, has a vapour pressure of 0,24 hPa [11]). A mixture of DMF and FA with a mass ratio of 1:5 was used for the laminating pastes. To reduce shrinkage of the precursor during pyrolysis with the addition of passive fillers, the polymer solutions were mixed with AlN powders (*H.C. Starck*, type C). This mixture was homogenized in four passes in a triple roll mill (speed = 350 min-1, smallest gap width ≙ 5 µm). Typical compositions are: DMF=10,1 mass %, FA=24,6 mass %, TMIA=14,1 mass %, AlN= 51,2 mass %. This corresponds to a volume ratio of the precursor to the AlN powder of 47:53.

For characterization of the rheological properties of the precursors and laminating pastes, a rotary viscometer (Viskotester VT550, *Haake Mess-Technik GmbH*) was used. The two systems MV-DIN and SV-DIN were used as measurement devices for medium-viscosity and higher viscosity substances respectively. All measurements were performed at 23°C. The mass loss during pyrolysis was determined by thermogravimetric analysis (STA 429, *Netzsch*). The heating rate was 10 K/min. The measurement was performed in a nitrogen atmosphere. Pyrolysis took place in a muffle furnace (type VMK-S 22, *Linn*), flushed with nitrogen. The non-cross-linked polymer must be heated very slowly to avoid foaming and a resulting excessive mass loss. The heating rate was 1 K/min. The maximum temperatures were 600 and 700°C.

The sintering tests were performed in a pressure sintering furnace type FPW, supplied by *FCT*). The heating rate was 10 K/min up to 1400°C and then 3 K/min up to 1800°C. The residence time at the final temperature of 1800°C was 30 min, at a nitrogen pressure of around 2 MPa. The laminates were sintered in an AlN powder bed in a C crucible. During sintering, the tapes were loaded with AlN plates, giving a pressure per unit area of around 40 g/cm².

The themperature conductivity was measured with a laser flash device (*ISC Würzburg*). One unlaminated single tape and three laminates of different thicknesses, each consisting of two individual tapes laminated with the rough tape surfaces on top of each other, were tested (samples A, B: single tape thickness = 1,3 mm, Sample C: single tape thickness = 0,5 mm). The measuredtemperatureconductivity a, the density r and the thermal capacity c can be used to calculate the thermal conductivity λ as follows:

$$\lambda = a \cdot \rho \cdot c$$

where: $\rho = 3{,}2\ g cm^{-3}$

$c = 738\ J kg^{-1} K^{-1}$

(specification provided by *ANCeram*)

Results and Discussion

Precursor Synthesis

The estimation of the concentration of TMIA in the synthesis solution after different synthesis times is based on the theoretical assumptions that no solvent loss nor cross-linking of the TMIA occurs as part of the chemical reactions that take place during the synthesis. During the electrolysis, the following subreactions take place [9]

$$Al \rightarrow Al^{3+} + 3e^-$$

$$3\ NH_2R + 3e^- \rightarrow 3\ NHR^- + 3/2\ H_2$$

The charge flowing per hour can be calculated from the current flow of I = 1,8 A = 1,8 C/s; charge per hour: F = 1,8 · 3600 C/h = 6480 C/h = $4{,}0 \cdot 10^{22}$ e⁻/h. Thus, per hour, $4 \cdot 10^{22}$ electrons and an equal number of molecules NHR are converted

Synthesis time [h]	10	13	15	24
Precursor concentration [%]	11,0	14,2	16,4	25,9
Al-solution [g]	6,0	7,8	9,0	14,4

Tab 1 Calculated concentrations of precursor TMIA in the synthesized solutions

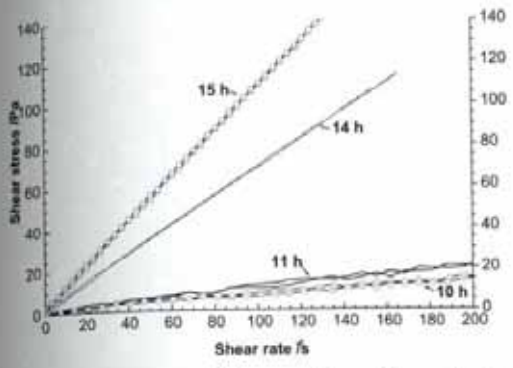

Fig. 4 (left)
Dependence of the shear stress versus shear rate for precursor solutions after different synthesis times

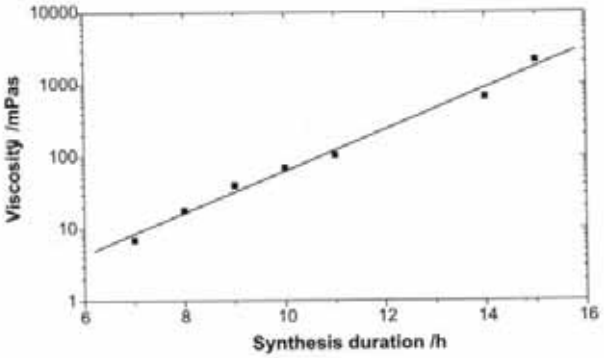

Fig. 5
Dependence of the viscosity of the precursor solutions versus synthesis duration (compensation straight lines calculated without the values of the 12- and 13-h synthesis solutions)

or 1/3 · 4 · 10^{22} atoms of Al are oxidized. That corresponds to 67 mmol NHR or 1/3 · 67 mmol Al^{3+} per hour. From the relative molar masses of the educts and products (propylamine = NH_2R with R = C_3H_7 or TMIA = $Al(NHR)_3$) it can be calculated that 3,97 g NH_2R (M=59,11 g/mol) are converted to 3,90 g NHR (M=58,19g/mol) in one hour. At the sametime, 0,60 g Al ions are formed. Therefore, in one hour, 4,50 g TMIA are produced.

From the starting composition, the respective precursor concentrations of the synthesis solution can be calculated from the values in Tab 1. The values determined only serve as an estimation of how high the concentration of TMIA can be at best after a certain synthesis time. Only after a time of 24 h does a quarter of the synthesized solution consist of precursor. In practice, however, there is a loss of solvent as a result of heating during electrolysis and, on the other hand, a saturation with increased synthesis time, so that the concentrations in the synthesized solution do not correspond exactly to the calculated values.

The precursor solutions synthesized over different lengths of time demonstrate clear differences in their viscosity. In all solutions, the shear rate D rises with the increasing shear stress in an almost linear function. Therefore they all demonstrate Newtonian behaviour (Fig. 4).

The different samples do not demonstrate a time-dependent behaviour. The upward and downward curves (increase or decrease of the speed of the viscometer and thus the shear stress) are virtually congruent. No hysteresis is formed. As the synthesis time is lengthened, the viscosity (slope of the straight lines in Fig. 4) increases considerably. The irregularities in the curve shape of the solutions synthesized at 10 and 11 h are attributed to the evaporation of the solvent and a "skin formation" at the surface of the measurement solution. With the increase in synthesis duration, the content of precursor in the solution rises. Moreover, the TMIA molecules are polymerized, leading to an exponential increase in the viscosity with increasing synthesis duration (Fig. 5).

Lamination, Drying and Sintering

Fig. 6 shows viscosity curves of different empirically optimized laminating pastes that only consist of partially cross-linked TMIA and the solvents. Apart from very low shear rates, the solutions demonstrate virtually Newtonian behaviour. No thixotropy can be detected.

Composition B proved the most suitable for the coating tests by means of screen printing as it contains the highest fraction of precursor. For the further tests, mixtures of the precursor and AlN powder were used to ensure a lower mass loss during pyrolysis and thus to obtain denser layers after pyrolysis and sintering. These pastes had a typical volume ratio between precursor and AlN of 47:53. The content of solvent was 53 vol. %.

The thermogravimetric analyses show that the pyrolysis of the cross-linked TMIA is completed at around 450°C (Fig. 7). In the non-cross-linked TMIA, NH_2R groups are still present and cause an additional mass loss during pyrolysis.

The total mass loss during pyrolysis is around 67 %. This corroborates the findings of Rüssel and Seibold [9]. In the case of the non-cross-linked TMIA, on the other hand, degradation is still not complete at 750°C. The mass loss at this temperature is around 80 %. The green tape consists of the ceramic powder and small quantities of organic additives. On heating, these organic components are also pyrolysed. The measured mass loss corresponds to the quantity of organic matter in the green tape. The mass loss of the AlN green tape (*ANCeram*) is around 9 % at 750°C (Fig. 7). The mass losses were taken into account in the elaboration of the temperature-time schedule for pyrolysis of the precursor and green tape and for sintering.

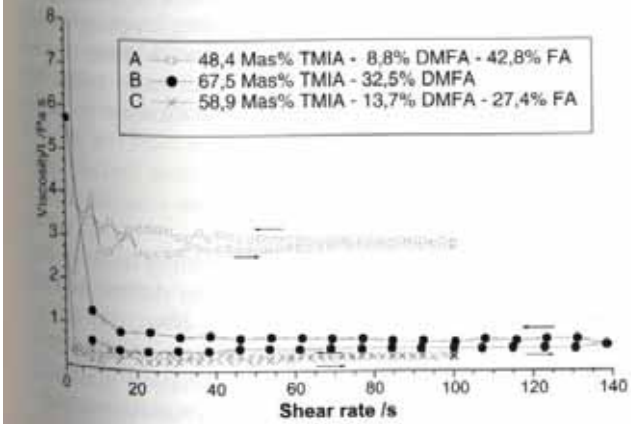

Fig. 6 (left)
Viscosity curves of different laminating pastes used for screen printing

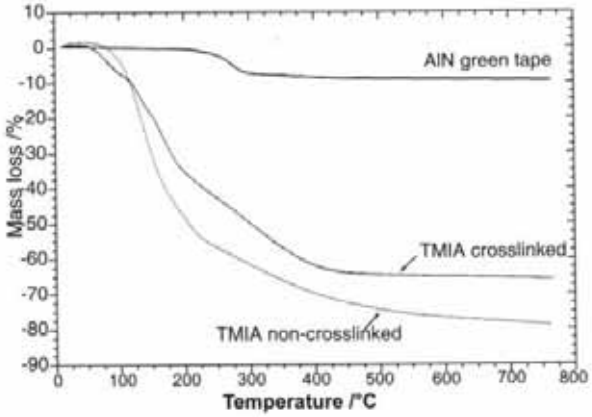

Fig 7
Mass loss of cross-linked and non-cross-linked TMIA in N_2 as well as AlN green tape; heating rate 10 K/min

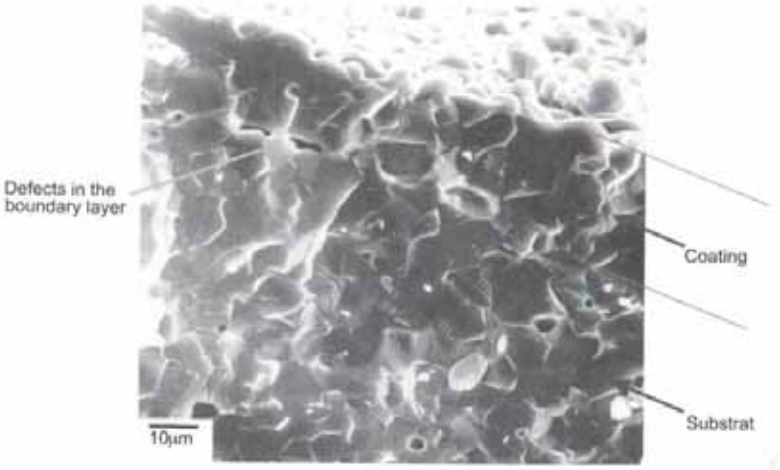

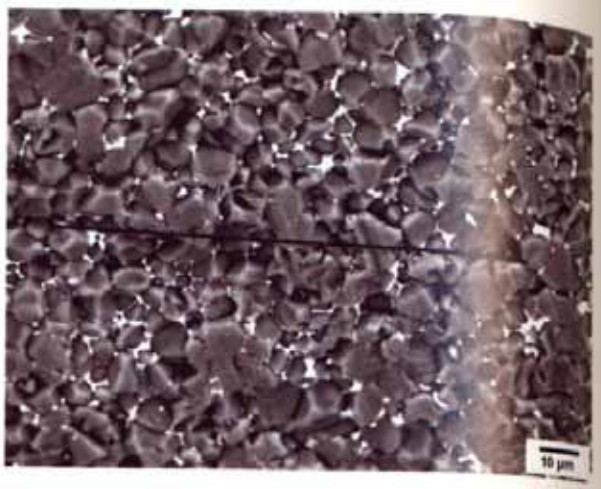

Fig. 8 (top left) Defects between the coating and the tape in the fracture surface of a precoated, pyrolysed and sintered tape (SEM, SE)

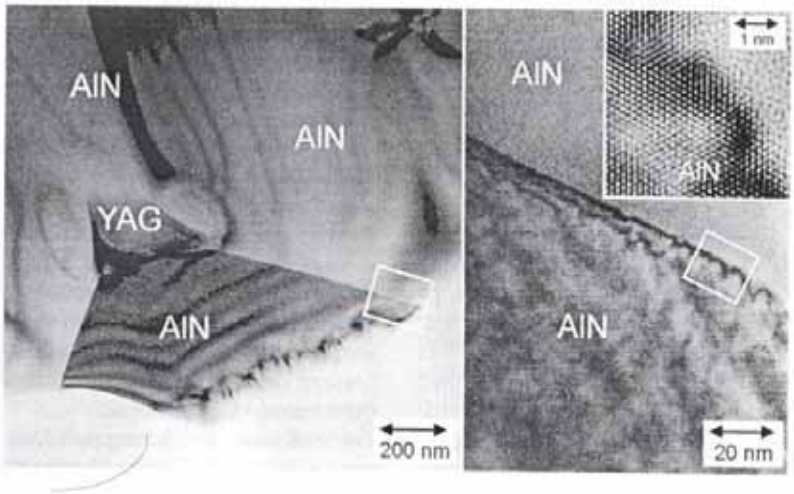

Fig. 9 (top right) Distribution of the high-yttrium phase in the fracture surface of a laminate produced by means of precoating (SEM, BSE)

Fig. 10 (below left) Concentration of the high-yttrium phase YAG ($Y_3Al_5O_{12}$) in triple points and grain boundaries free of amorphous grain boundary phase in the region around the laminating layer in a laminate produced by means of precoating (TEM)

Microstructure and Properties

For a green tape coated on one side with a 13-h synthesis solution, a layer thickness of < 20 µm (Fig. 8) is formed after sintering. The microstructure of the coating is similar to that of the substrate. The borderline between the coating and the substrate is only recognizable at defects, e.g. pores, between the coating and the substrate (Fig. 8, left). The laminates exhibit areas in which differences or interfaces between the different tapes cannot be recognized either with the naked eye nor with higher magnification SEM. Often, however, these areas are interrupted by delaminations or areas of increased porosity. The microstructure consists of isomorphic particles with a diameter of several micrometres.

The yttria added as a sintering aid leads to liquid phase sintering of the AlN. After sintering, this melt phase concentrates in triple points and can be identified in the backscattered SEM image as a light-coloured secondary phase (Fig. 9). The laminating point is indicated by a black line in Fig. 9. There is no difference between the grain size distribution in the tape and that in the laminating layer. The laminating layer originally consists only of the pyrolysed AlN precursor without the addition of yttria. Nevertheless, the yttria-containing phase can also be found in the laminating layer region, although partly in a lower concentration. During the sintering process, therefore, the low-viscous, high-yttrium secondary phase moves along the grain boundaries into the laminating layer region, which explains why the microstructure of the laminating layer hardly differs from that of the tape.

The concentration of the secondary phase mainly in the triple points and not at the grain boundaries can also be clearly seen in the high-resolution transmission electron microscope image shown in Fig. 10. The grain boundaries are free of secondary phases and exhibit a crystalline structure.

Thermal Conductivity

The thermal conductivity of AlN is strongly dependent on the purity and microstructure of the material. Defects in the crystal structure, caused, for example, by O atoms instead of N atoms in the crystal lattice, lead to increased phonon scattering and thus to lower conductivity [12,13]. The addition of yttrium causes during sintering the formation of a secondary phase along the grain boundaries and primarily in the grain triple points. In this secondary phase, the contaminants from the AlN grains are dissolved, which causes an increase in the thermal conductivity of the material [14].

As the measured values for the laminates show, the laminating layer reduces thermal conductivity (Tab 2). The samples exhibit numerous defects in the laminating layer and these hinder heat transfer severely. The object of further tests will be to apply the laminating layers without any defects and to work under cleaner ambient conditions in order to effect a substantial increase in thermal conductivity.

Tab 2 Thermal properties of the laminates (all values at AT)

Sample	Thickness [%]	Temperature conductivity [mm^2s^{-1}]	Thermal conductivity [$Wm^{-1}K^{-1}$]
Single tape	0,74	44	106
Two-ply laminate (A)	1,69	30	71
Two-ply laminate (B)	1,64	23	56
Two-ply laminate (thin green tapes C)	0,78	16	38

Prospects

In defect free laminating layers of the tape microstructures do not exhibit any differences after sintering. Therefore, with the use of an AlN precursor as laminating paste, it seems possible to produce multilay-

components with no or only slight differences in their properties perpendicular and parallel to the laminating layers.

Acknowledgement

This research was kindly supported by the German Ceramic Society (DKG) trough the *Arbeitsgemeinschaft industrieller Forschungsgemeinschaften (AIF)* with funds from the German Ministry for Economics under AIF No. 11401N. The authors also wish to thank Dr. *H. Giebe* (University of Bayreuth) for performing the SEM and TEM analyses.

References

[1] M. Güther, K. Seitz: Kühlung mit Keramik. Future Special Science **1** (1995) 28-31

[2] F. Klocke, O. Gerent, C. Schippers: Green Maschining-Economical and Technical Potentials. Production Engineering Vol. III/1 (1996) 15-18

[3] J.G. Heinrich: New Developments in the Solid Freeform Fabrication of Ceramic Components. cfi/Ber.DKG **76** (1999) 29-35

[4] G. Kleer, R. Goller, W. Döll, J. Heinrich, O. Rosenfelder: Strength and Crack Propagation Behaviour of Anisotropic Laminated SiSiC. Proc. 2nd Conf. Eur. Ceram. Soc. 1991, September 11-14, Augsburg, Germany 1-5

[5] G. Kleer, H. Richter, G. Willmann, W. Heider, G. Popp: Bruchmechanische Charakterisierung des Ermüdungsverhaltens von SiSiC. Z. Werkstofftech. **16** (1985) 94-101

[6] J.G. Heinrich: Foliengießen oxidischer und nichtoxidischer keramischer Pulver. Keramische Zeitschrift 2 (1986), 79-82.

[7] M. Seibold, C. Rüssel: A Novel Route to Aluminium Nitride Ceramics Using a Polyiminoalane Precursor. Mat.Res.Soc.Symp.Proc. **121**, 1988, 477-482

[8] M. Seibold, U. Vierneusel, C. Rüssel: Aluminium Nitride Ceramics Prepared by a Polymeric Precursor. Ceramic Powder Processing Science, Proc. 2nd Int. Conf., Berchtesgaden, Germany, October 12-14, 1988 173-179

[9] M. Seibold, C. Rüssel: Thermal Conversion of Preceramic Polyiminoalane Precursors to Aluminium Nitride: Characterization of Pyrolysis Products. J.Am.Ceram.Soc. **72** (1989) 1503-1505

[10] C. Rüssel, M. Seibold: Verfahren zur Herstellung von für keramische Materialien geeigneten Nitriden, die nach dem Verfahren hergestellten Nitride sowie deren Verwendung. Patentschrift DE 38 07 419 C2 (Veröffentlichungstag: 12.4.90).

[11] ChemDat, Chemie-Datenbank 99'1 D, Merck AG

[12] A. Kranzmann and S. Ruckmich: Aluminiumnitridkeramik, in: DKG - Technische keramische Werkstoffe, J. Kriegesmann (Hrsg.), Dt. Wirtschaftsdienst, Köln 1992, Kap. 4.3.4.0, S.1-42

[13] J. Jarrige, J. P. Lecompte, J. Mullot, and G. Müller: Effect of Oxygen on the Thermal Conductivity of Aluminum Nitride Ceramics, J.Eur.Ceram.Soc. **17** (1997) 1891-1895

[14] P. Sainz de Baranda, A.K. Knudsen, E. Ruh: Effect of Yttria on the Thermal Conductivity of Aluminum Nitride, J.Am.Ceram.Soc. **77** (1994) 1846-50

[15] G. Himpel and I. Haase: Entwicklung von AlN-Keramik hoher Wärmeleitfähigkeit, cfi/Ber. DKG **69** (1992) 466-472